1-D non-periodic homogenization for the seismic wave equation

Yann Capdeville, Laurent Guillot, Jean-Jacques Marigo

HAL Id: hal-00538413
https://hal.science/hal-00538413

Submitted on 16 Jun 2017

1-D non-periodic homogenization for the seismic wave equation

Yann Capdeville,[1] Laurent Guillot[1] and Jean-Jacques Marigo[2]

[1]*Équipe de sismologie, Institut de Physique du Globe de Paris (*UMR 7154*), CNRS. E-mail: capdevil@ipgp.jussieu.fr*
[2]*Laboratoire de Mécanique des solides (*UMR 7649*), École Polytechnique, Palaiseau, France*

SUMMARY
When considering numerical acoustic or elastic wave propagation in media containing small heterogeneities with respect to the minimum wavelength of the wavefield, being able to upscale physical properties (or homogenize them) is valuable mainly for two reasons. First, replacing the original discontinuous and very heterogeneous medium by a smooth and more simple one, is a judicious alternative to the necessary fine and difficult meshing of the original medium required by many wave equation solvers. Second, it helps to understand what properties of a medium are really 'seen' by the wavefield propagating through, which is an important aspect in an inverse problem approach. This paper is an attempt of a pedagogical introduction to non-periodic homogenization in 1-D, allowing to find the effective wave equation and effective physical properties, of the elastodynamics equation in a highly heterogeneous medium. It can be extrapolated from 1-D to a higher space dimensions. This development can be seen as an extension of the classical two-scale homogenization theory applied to the elastic wave equation in periodic media, with this limitation that it does not hold beyond order 1 in the asymptotic expansion involved in the classical theory.

Key words: Computational seismology; Wave scattering and diffraction; Wave propagation.

1 INTRODUCTION

In seismology or in seismic exploration, inhomogeneities of scale much smaller than the minimum wavelength are a challenge for both the forward problem and the inverse problem. This introduction is focused on the forward problem.

In recent years, advances in numerical methods have allowed to model full seismic waveforms in complex media. Among these advances in numerical modelling, the introduction of the Spectral Element Method (SEM) (see, for example, Priolo *et al.* 1994; Komatitsch & Vilotte 1998, for the first SEM applications to the elastic wave equation and Chaljub *et al.* 2007 for a review) has been particularly interesting. This method has the advantage to be accurate for all kinds of waves and any type of media, as long as a hexahedral mesh, on which the method most often relies, can be designed for a partition of the space (note the SEM can be based on tetrahedral meshes Komatitsch *et al.* 2001; Mercerat *et al.* 2006, but at the price of lower efficiency). This method can be very efficient, depending on the complexity of the mesh. Nevertheless, difficulties arise when encountering some spatial patterns quite typical of the Earth like 0th-order discontinuities in material properties.

Time signals in seismology, recorded at some receivers after the Earth has been excited (e.g. by some quake), have a finite frequency support $[f_{min}, f_{max}]$. This finiteness can be due to the instrument response at the receiver, to the limited frequency band of the source, to the attenuation in the medium, or to the bandpass filtering applied to the data by a seismologist. For the wave equation, the existence of a frequency cut-off f_{max} of a wavefield propagating in a medium implies the existence of a minimum wavelength for this wavefield except in some special locations (close to a point source for example). The knowledge of this maximum frequency—and of the associated, minimum wavelength—allows to efficiently solve the wave equation with numerical techniques like the SEM, in some complex media, at a reasonable cost. Indeed, when the medium is smoothly heterogeneous and does not contain scales smaller than the minimum wavelength of the wavefield, the mesh design is mostly driven by the sampling of the wavefield and the numerical cost is minimum. On the other hand, when the medium contains heterogeneities at a small scale, the mesh design is driven by the sampling of these heterogeneities, and this can lead to a very high numerical cost. Another constraint on the mesh design is that all physical discontinuities must be matched by an element interface. If for technical reasons, a mesh honouring all physical interfaces cannot be designed, the accuracy of the numerical solution is not warranted and even worse, for special waves like interface waves, the accuracy is difficult to be predicted. In realistic 3-D media, an hexahedral mesh design is often impossible and requires simplifications in the model structure. Despite this trick, once the mesh is designed, its complexity again involves a very small time step to satisfy the stability condition of the explicit Newmark time scheme used in most cases (Hughes 1987), leading to a very high numerical cost. This time step problem can be avoided with unconditionally stable time schemes (Seriani 1997, 1998), but at a price of a higher complexity and numerical cost and such schemes are not widely

GJI Seismology

used so far. Let us mention that other methods based on tetrahedral meshes (whose design is much simpler than hexahedral ones and can be automated) like the ADER scheme (Kaser & Dumbser 2006) or SEM based on tetrahedral meshes (Komatitsch *et al.* 2001; Mercerat *et al.* 2006) exist, are promising, but so far less competitive than the hexahedral version of SEM.

There is an alternative way to overcome these technical problems. It is based on simple physical considerations, and intimately connected to the reason why we are able to model seismic data quite simply in some situations. Indeed it is known (see, for example, Backus 1962; Chapman 2004, or the work on highly heterogeneous media of Zhang & LeVeque 1997; Fogarty & LeVeque 1999) that heterogeneities whose size is much smaller than the minimum wavelength, only affect the wavefield in an effective way, and this is why simple models can be very efficient to predict data in some cases. A pertinent example is given in global seismology: very long period data can be predicted with a good accuracy using a simple spherically symmetric model, despite the relatively well-known complex structure in the crust at smaller scales. Being aware of this fact, and rather than trying to mesh details much smaller than the minimum wavelength of a wavefield, an appealing idea is to find a smooth, effective model (and as we shall see, an effective wave equation) that would lead to an accurate modelling of data, without resorting to a very fine partition of the space. The issue is then the following: given a known acoustic or elastic model, containing heterogeneities at scales much smaller that the minimum wavelength of a wavefield propagating through, may one find a smooth effective model and an effective wave equation, that reproduce the full waveform observed in the original medium? In other words, how may one upscale the original medium to the scale of the wavefield?

In the static case, this kind of problem has been studied for a long time and a large number of results have been obtained using the so-called homogenization theory applied to media showing rapid and periodical variations of their physical properties. Since the pioneering work of Auriault & Sanchez-Palencia (1977), numerous studies have been devoted either to the mathematical foundations of the homogenization theory in the static context (e.g. Bensoussan *et al.* 1978; Murat & Tartar 1985; Allaire 1992), to applications to the effective static behaviour of composite materials (e.g. Dumontet 1986; Francfort & Murat 1986; Abdelmoula & Marigo 2000; Haboussi *et al.* 2001a,b), to the application to the heat diffusion (e.g. Marchenko & Khruslov 2005), to porous media (e.g. Hornung 1996), etc. In contrast, fewer studies have been devoted to the theory and its applications in the general dynamical context or to the non-periodic cases. However, one can for example refer to Sanchez-Palencia (1980), Willis (1981), Auriault & Bonnet (1985), Moskow & Vogelius (1997), Allaire & Conca (1998), Fish *et al.* (2002), Fish & Chen (2004), Parnell & Abrahams (2006), Milton & Willis (2007), Lurie (2009) or Allaire *et al.* (2009) for the dynamical context, to Briane (1994), Nguetseng (2003) or to Marchenko & Khruslov (2005) for the non-periodic case. Moczo *et al.* (2002) have also used a kind of local homogenization to take into account interfaces with the finite differences method. The specific case of a long wave propagating in finely layered media has been studied by Backus (1962) and the same results can be extracted from the 0th-order term of the asymptotic expansion implied in homogenization theory. Higher order homogenization in the non-periodic case has been studied by Capdeville & Marigo (2007) and Capdeville & Marigo (2008) for wave propagation in stratified media, but the extension to media characterized by 3-D rapid variation is not obvious from these works. Indeed, the non-periodic homogenization strategy suggested in Capdeville & Marigo (2007)

is based on the knowledge of an explicit solution of the cell problem (see main text for a definition of this concept), and such a solution only exists for layered media. The challenge is therefore to present a non-periodic homogenization that can be extended from the 1-D to the 2-D/3-D case.

We first recall some general features of the homogenization theory in the context of 1-D periodic media, in a slightly different manner as done by Fish *et al.* (2002). Then, we generalize these results, to 1-D non-periodic media in a way that can be extended form 1-D to 2-D/3-D. Numerical convergence tests of the asymptotic, homogenized solution towards the reference one, are performed. Our aim is to present in this paper, a clear introduction for the 1-D case, of the techniques and hypotheses that will be presented later for 2-D and 3-D wave propagation problems.

2 1-D PERIODIC CASE

We consider an infinite elastic bar of density ρ^0 and elastic modulus E^0. In this first part, it is assumed that the bar properties are ℓ-periodic, that is $\rho^0(x + \ell) = \rho^0(x)$ and $E^0(x + \ell) = E^0(x)$. The bar is considered as infinite in order to avoid the treatment of any boundary condition that normally would be necessary in the following development. The boundary condition problem associated with homogenization has nevertheless been addressed by Capdeville & Marigo (2007) and Capdeville & Marigo (2008) for layered media, and will be the purpose of future works for a more general case. An external force $f = f(x, t)$ is applied to the bar inducing a displacement field $u(x, t)$ propagating along the x axis. We assume that $f(x, t)$ has a corner frequency f_c which allows us to assume that a minimum wavelength λ_m to the wavefield u exists. The main assumption of this section is

$$\varepsilon = \frac{\ell}{\lambda_m} \ll 1 \tag{1}$$

which means that the size of heterogeneities in the bar is much smaller than the minimum wavelength of the propagating wavefield.

2.1 Set up of the homogenization problem

In this section, we give an intuitive construction of the homogenization problem. For a more precise and formal set up, one can for example refers to Sanchez-Palencia (1980). A classical homogenization problem is built over a sequence of problems obtained by varying the periodicity ℓ. For a fixed λ_m, one particular bar model of periodicity ℓ is associated to a unique ε and therefore, the sequence of problems can be indexed by the sequence of ε. The original problem, which has a given periodicity, let say ℓ_0, corresponding to the parameter $\varepsilon_0 = \ell_0/\lambda_m$, is met only if $\varepsilon = \varepsilon_0$. To the sequence of problems corresponds a sequence of elastic and density properties named E^ε and ρ^ε (and we have $E^{\varepsilon_0} = E^0$ and $\rho^{\varepsilon_0} = \rho^0$). We assume the external source does not depend on ε. Nevertheless, in practice, the source if often represented as a point source which can lead to some complications. This point will be discussed and addressed at the end of this section. We assume here that f is smooth both in space and time. For a given ε, the equation of motion and constitutive relation in the bar are

$$\begin{aligned}\rho^\varepsilon \partial_{tt} u^\varepsilon - \partial_x \sigma^\varepsilon &= f \\ \sigma^\varepsilon &= E^\varepsilon \partial_x u^\varepsilon,\end{aligned} \tag{2}$$

where $u^\varepsilon = u^\varepsilon(x, t)$ is the displacement along x, $\sigma^\varepsilon = \sigma^\varepsilon(x, t)$ is the stress, $\partial_{tt} u^\varepsilon$ the second derivative of u^ε with respect to time and
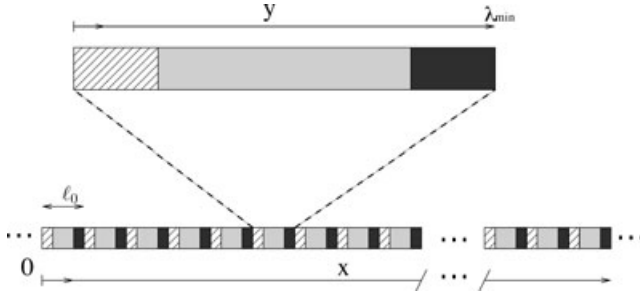
Figure 1. Sketch showing the infinite periodic bar and a zoom on one periodic cell.

∂_x the partial derivative with respect to x. We assume zero initial conditions at $t = 0$ and radiation conditions at the infinity.

To explicitly take small-scale heterogeneities into account when solving the wave equation, a fast space variable is introduced (see Fig. 1)

$$y = \frac{x}{\varepsilon}, \tag{3}$$

where y is called the microscopic variable and x is the macroscopic variable. When $\varepsilon \to 0$, any change in y induces a very small change in x. This leads to the separation of scales: y and x are treated as independent variables. This implies that partial derivatives with respect to x become

$$\frac{\partial}{\partial x} \to \frac{\partial}{\partial x} + \frac{1}{\varepsilon} \frac{\partial}{\partial y}. \tag{4}$$

The solution to the wave eqs (2) is sought as an asymptotic expansion in ε

$$u^{\varepsilon}(x, t) = \sum_{i \geq 0} \varepsilon^i u^i(x, x/\varepsilon, t) = \sum_{i \geq 0} \varepsilon^i u^i(x, y, t),$$
$$\sigma^{\varepsilon}(x, t) = \sum_{i \geq -1} \varepsilon^i \sigma^i(x, x/\varepsilon, t) = \sum_{i \geq -1} \varepsilon^i \sigma^i(x, y, t), \tag{5}$$

in which coefficients u^i and σ^i depend on both space variables x and y and must be λ_m-periodic in y. This ansatz—the x and y dependence of the solution—explicitly incorporates our intuition, that the sought solution, depends on the wavefield at the large scale, but also, locally, on the fast variations of elastic properties. Starting the stress expansion at $i = -1$ is required by constitutive relation between the stress and the displacement and the $1/\varepsilon$ in (4).

We introduce ρ and E

$$\rho(y) = \rho^{\varepsilon}(\varepsilon y),$$
$$E(y) = E^{\varepsilon}(\varepsilon y), \tag{6}$$

the unit cell elastic modulus and density. E and ρ are independent of ε and are λ_m-periodic. Introducing expansions (5) in eqs (2), using (4) and identifying term by term in ε^i we obtain:

$$\rho \partial_{tt} u^i - \partial_x \sigma^i - \partial_y \sigma^{i+1} = f \delta_{i,0}, \tag{7}$$

$$\sigma^i = E \left(\partial_x u^i + \partial_y u^{i+1} \right), \tag{8}$$

where $\delta_{i,0}$ takes for value 1 for $i = 0$ and 0 otherwise. These last equations have to be solved for each i. Before going further, we introduce the cell average, for any function $h(x, y)$ λ_m-periodic in y

$$\langle h \rangle (x) = \frac{1}{\lambda_m} \int_0^{\lambda_m} h(x, y) \mathrm{d}y. \tag{9}$$

For any function $h(x, y)$, λ_m-periodic in y, it can easily be shown that

$$\partial_y h = 0 \Leftrightarrow h(x, y) = \langle h \rangle (x), \tag{10}$$

and

$$\langle \partial_y h \rangle = 0. \tag{11}$$

2.2 Resolution of the homogenization problem

In the following, the time dependence t is dropped to ease the notations.

- Eqs (7) for $i = -2$ and (8) for $i = -1$ give

$$\partial_y \sigma^{-1} = 0,$$
$$\sigma^{-1} = E \partial_y u^0, \tag{12}$$

which implies

$$\partial_y \left(E \partial_y u^0 \right) = 0. \tag{13}$$

Multiplying the last equation by u^0, integrating over the unit cell, using an integration by part and taking account of the periodicity of u^0 and $E \partial_y u^0$, we get

$$\int_0^{\lambda_m} \left(\partial_y u^0 \right)^2 E \, \mathrm{d}y = 0. \tag{14}$$

$E(y)$ being a positive function, the unique solution to the above equation is $\partial_y u^0 = 0$. We therefore have

$$u^0 = \langle u^0 \rangle, \tag{15}$$

$$\sigma^{-1} = 0. \tag{16}$$

Eq. (15) implies that the order 0 solution in displacement is independent on the fast variable y. This is an important result that confirms the well known fact that the displacement field is poorly sensitive to scales much smaller than its own scale.

- Eqs (7) for $i = -1$ and (8) for $i = 0$ give

$$\partial_y \sigma^0 = 0, \tag{17}$$

$$\sigma^0 = E \left(\partial_y u^1 + \partial_x u^0 \right). \tag{18}$$

Eq. (17) implies that $\sigma^0(x, y) = \langle \sigma^0 \rangle(x)$ and, with (18), that

$$\partial_y \left(E \partial_y u^1 \right) = -\partial_y E \, \partial_x u^0. \tag{19}$$

Using the linearity of the last equation we can separate the variables and look for a solution of the form

$$u^1(x, y) = \chi^1(y) \partial_x u^0(x) + \langle u^1 \rangle(x), \tag{20}$$

where $\chi^1(y)$ is called the first-order periodic corrector. To enforce the uniqueness of the solution, we impose $\langle \chi^1 \rangle = 0$. Introducing (20) into (19), we obtain the equation of the so-called cell problem

$$\partial_y \left[E \left(1 + \partial_y \chi^1 \right) \right] = 0, \tag{21}$$

χ^1 being λ_m-periodic and verifying $\langle \chi^1 \rangle = 0$. It is useful to note that a general analytical solution to (21) exists and is

$$\chi^1(y) = -y + a \int_0^y \frac{1}{E(y')} \mathrm{d}y' + b. \tag{22}$$

The periodicity condition imposes

$$a = \left\langle \frac{1}{E} \right\rangle^{-1}, \tag{23}$$

and b can be found using $\langle \chi^1 \rangle = 0$. We therefore have

$$\partial_y \chi^1(y) = -1 + \left\langle \frac{1}{E} \right\rangle^{-1} \frac{1}{E(y)}. \tag{24}$$

Introducing (20) into (18), taking the cell average and using the fact that we have shown that σ^0 does not depend upon y, we find the order 0 constitutive relation,

$$\sigma^0 = E^* \partial_x u^0 \,, \tag{25}$$

where E^* is the order 0 homogenized elastic coefficient,

$$E^* = \left\langle E \left(1 + \partial_y \chi^1\right)\right\rangle \,. \tag{26}$$

Using (24) in the last equation we have

$$E^* = \left\langle \frac{1}{E}\right\rangle^{-1} \,. \tag{27}$$

- Eqs (7) for $i = 0$ and (8) for $i = 1$ give

$$\rho \partial_{tt} u^0 - \partial_x \sigma^0 - \partial_y \sigma^1 = f, \tag{28}$$

$$\sigma^1 = E \left(\partial_y u^2 + \partial_x u^1\right). \tag{29}$$

Applying the cell average on (28), using the property (11), the fact that u^0 and σ^0 do not depend on y and gathering the result with (25), we find the order 0 wave equation

$$\rho^* \partial_{tt} u^0 - \partial_x \sigma^0 = f$$
$$\sigma^0 = E^* \partial_x u^0 \,, \tag{30}$$

where $\rho^* = \langle \rho \rangle$ is the effective density and E^* is defined by eq. (27). This is the classical wave equation that can be solved using classical techniques. Knowing that ρ^* and E^* are constant, solving the wave equation for the order 0 homogenized medium is a much simpler task than for the original medium and no numerical difficulty related to the rapid variation of the properties of the bar arises. One of the important results of homogenization theory is to show that u^ε 'converges' to u^0 when ε tends towards 0 (the so-called convergence theorem, see Sanchez-Palencia 1980).

Once u^0 is found, the first-order correction, $\chi^1(x/\varepsilon) \partial_x u^0(x)$, can be computed. To obtain the complete order 1 solution u^1 using (20), $\langle u^1 \rangle$ remains to be found. Subtracting (30) from (28) we have,

$$\partial_y \sigma^1 = (\rho - \langle \rho \rangle)\partial_{tt} u^0 \,, \tag{31}$$

which, together with (29) and (20) gives

$$\partial_y \left(E \partial_y u^2\right) = -\partial_y \left(E \partial_x u^1\right) + (\rho - \langle \rho \rangle)\partial_{tt} u^0 \,, \tag{32}$$

$$= -\partial_y E \, \partial_x \langle u^1 \rangle - \partial_y (E \chi^1)\partial_{xx} u^0 + (\rho - \langle \rho \rangle)\partial_{tt} u^0 \,. \tag{33}$$

Using the linearity of the last equation we can separate the variables and look for a solution of the form

$$u^2(x,y) = \chi^2(y)\partial_{xx} u^0(x) + \chi^1(y)\partial_x \langle u^1 \rangle(x) + \chi^\rho(y)\partial_{tt} u^0(x) + \langle u^2 \rangle(x), \tag{34}$$

where χ^2 and χ^ρ are solutions of

$$\partial_y \left[E \left(\chi^1 + \partial_y \chi^2\right)\right] = 0 \,, \tag{35}$$

$$\partial_y \left[E \partial_y \chi^\rho\right] = \rho - \langle \rho \rangle \,, \tag{36}$$

with χ^2 and χ^ρ λ_m-periodic and where we impose $\langle \chi^2 \rangle = \langle \chi^\rho \rangle = 0$ to ensure the uniqueness of the solutions. Introducing (34) into (29) and taking the cell average, we find the order 1 constitutive relation

$$\langle \sigma^1 \rangle = E^* \partial_x \langle u^1 \rangle + E^{1*} \partial_{xx} u^0 + E^{\rho*} \partial_{tt} u^0 \tag{37}$$

with

$$E^{1*} = \left\langle E \left(\chi^1 + \partial_y \chi^2\right)\right\rangle \tag{38}$$

$$E^{\rho*} = \left\langle E \partial_y \chi^\rho \right\rangle \,. \tag{39}$$

The periodicity condition on χ^2 imposes $\partial_y \chi^2 = -\chi^1$ and therefore $E^{1*} = 0$.

Finally using (20) and taking the average of eqs (7) for $i = 1$ gives the order 1 wave equation

$$\langle \rho \rangle \partial_{tt} \langle u^1 \rangle + \langle \rho \chi^1 \rangle \partial_x \partial_{tt} u^0 - \partial_x \langle \sigma^1 \rangle = 0$$
$$\langle \sigma^1 \rangle = E^* \partial_x \langle u^1 \rangle + E^{\rho*} \partial_{tt} u^0 \,. \tag{40}$$

It is shown in the Appendix that $E^{\rho*} = \langle \rho \chi^1 \rangle$ and therefore, renaming $\langle \tilde{\sigma}^1 \rangle = \langle \sigma^1 \rangle - E^{\rho*} \partial_{tt} u^0$, the last equations can be simplified to

$$\langle \rho \rangle \partial_{tt} \langle u^1 \rangle - \partial_x \langle \tilde{\sigma}^1 \rangle = 0$$
$$\langle \tilde{\sigma}^1 \rangle = E^* \partial_x \langle u^1 \rangle \,. \tag{41}$$

We stop here our resolution but we could go up to a higher order (see Fish *et al.* 2002, for a 1-D periodic case up to the order 2).

2.3 Combining all orders together

Our aim is to solve for the homogenized wave equation using numerical methods like the Spectral Element Method (SEM). For such a method it is convenient to combine all the orders together rather than solving each order one after another. For that purpose, we solve for $\langle \hat{u}^{\varepsilon,1} \rangle$ solution of

$$\langle \rho \rangle \partial_{tt} \langle \hat{u}^{\varepsilon,1} \rangle - \partial_x \langle \hat{\sigma}^{\varepsilon,1} \rangle = f \tag{42}$$

$$\langle \hat{\sigma}^{\varepsilon,1} \rangle = E^* \partial_x \langle \hat{u}^{\varepsilon,1} \rangle \,. \tag{43}$$

One can check that

$$\langle \hat{u}^{\varepsilon,1} \rangle = u^0 + \varepsilon \langle u^1 \rangle + O(\varepsilon^2) \,, \tag{44}$$

$$\langle \hat{\sigma}^{\varepsilon,1} \rangle = \sigma^0 + \varepsilon \langle \tilde{\sigma}^1 \rangle + O(\varepsilon^2) \,. \tag{45}$$

Furthermore, if we name

$$\hat{u}^{\varepsilon,1} = \left[1 + \varepsilon \chi^1 \left(\frac{x}{\varepsilon}\right) \partial_x\right] \langle \hat{u}^{\varepsilon,1} \rangle \tag{46}$$

we can show that

$$\hat{u}^{\varepsilon,1} = u^\varepsilon + O(\varepsilon^2) \,. \tag{47}$$

Higher order terms in the asymptotic expansion can be added, as it will be shown below for the partial order 2.

2.4 External point sources

In practice, the external source is often localized to an area much smaller than the smallest wavelength λ_m allowing to consider it ideally as a point source: $f(x, t) = g(t)\delta(x - x_0)$. Two potential issues then arise:

(i) In the vicinity of x_0, there is no such a thing as a minimum wavelength. The asymptotic development presented here is therefore only valid far away enough from x_0.

(ii) A point source has a local interaction with the microscopic structure that needs to be accounted for.

The first point is not really a problem because, for most realistic cases, the point source assumption is not valid in the near field anyway. One should nevertheless keep in mind that very close to x_0, which means closer than λ_m, the solution is not accurate but not less than any standard numerical methods used to solve the
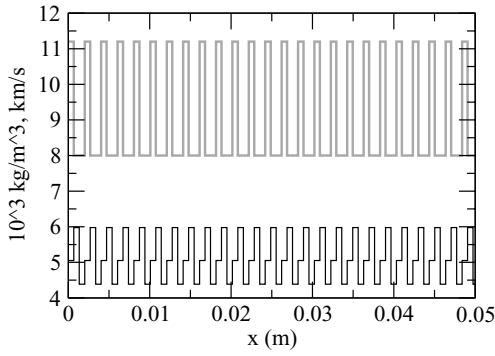
Figure 2. Sample (5 cm) of the bar density (grey line, in 10^3 kg m^{-3}) and velocity (black line, in km s^{-1}) for $l_0 = 6$ mm.

wave equation. The second point is more important and can be addressed the following way: the hypothetical point source is just a macroscopic representation of a more complex physical process, and what is relevant is to ensure the conservation of the energy released at the source. Therefore we need to find an effective source $\hat{f}^{\varepsilon,1}$ that preserves the energy associated to the original force f up to the wanted order (here 1). We therefore need

$$(u^\varepsilon, f) = (\langle \hat{u}^{\varepsilon,1} \rangle, \hat{f}^{\varepsilon,1}) + O(\varepsilon^2), \tag{48}$$

where $(.,.)$ is the L^2 inner product, and, for any function g and h is

$$(g, h) = \int_\mathbb{R} g(x)h(x)\mathrm{d}x. \tag{49}$$

Using (47), (46) and an integration by part, we find

$$\hat{f}^{\varepsilon,1}(x, t) = \left[1 - \varepsilon \chi^1 \left(\frac{x}{\varepsilon}\right) \partial_x\right] f(x, t). \tag{50}$$

$\hat{f}^{\varepsilon,1}$ needs to be used in (42) instead of f.

2.5 A numerical experiment for a periodic case

A numerical experiment in a bar of periodic properties shown in Fig. 2 is performed. The periodicity of the structure is $l_0 = 6$ mm.

First, the cell problems (21), (35) and (36) with periodic boundary conditions are solved with a finite element method based on the same mesh and quadrature than the one that will be used to solve the wave equation. This is not necessary, but for this simple 1-D case, it is a convenient solution. This allows to compute E^*, the correctors χ^1, χ^2 and χ^ρ as well as the external source term $\hat{f}^{\varepsilon,1}$. Then, the homogenized wave equation,

$$\langle \rho^0 \rangle \partial_{tt} u - \partial_x (E^* \partial_x u) = f, \tag{51}$$

where $u = \langle \hat{u}^{\varepsilon,1} \rangle$ and $f = \hat{f}^{\varepsilon,1}$, is solved using the SEM (see Capdeville 2000, for a complete description of the 1-D SEM).

A point source is located at $x = 2$ m. The time wavelet $g(t)$ is a Ricker with a central frequency of 50 kHz (which gives a corner frequency of about 125 kHz) and a central time shift $t_0 = 6.4 \times 10^{-5}$ s. In the far field, this wavelet gives a minimum wavelength of about 4 cm; that corresponds to a wave propagation with $\varepsilon = 0.15$. In practice the bar is of course not infinite, but its length (5 m) and the time (4.9×10^{-4} s) at which is recorded the displacement is such that the wave pulse does not reach the extremity of the bar. To be accurate, the reference solution is computed with a SEM mesh matching all interfaces with an element boundary (7440 elements for the 5 m bar). To make sure that only the effect of homogenization is seen in the simulations, the mesh and time step used to compute the reference solution are also used to compute the

homogenized solutions. Once the simulation is done, for a given time step corresponding to $t = 4.9 \times 10^{-4}$ s, the complete order 1 solution can be computed with (46). We can also compute the incomplete homogenized solution at the order 2

$$\hat{u}^{\varepsilon,3/2} = \left[1 + \varepsilon \chi^1 \left(\frac{x}{\varepsilon}\right) \partial_x + \varepsilon^2 \chi^2 \left(\frac{x}{\varepsilon}\right) \partial_{xx} + \varepsilon^2 \chi^\rho \left(\frac{x}{\varepsilon}\right) \partial_{tt}\right] \\ \times \langle \hat{u}^{\varepsilon,1} \rangle, \tag{52}$$

where $\hat{u}^{\varepsilon,3/2}$ is an incomplete order 2 solution and the '3/2' is just a notation to indicate that it is the order 1 plus second order correction ('1/2 order 2'). It is incomplete because $\langle u^2 \rangle$ has not been computed and is missing in (52) to obtain $\hat{u}^{\varepsilon,2}$. In other words, $\hat{u}^{\varepsilon,3/2}$ only contains the order 2 periodic correction beyond the order 1 solution.

In Fig. 3 are shown the results of the simulation. On the upper left plot (Fig. 3a) are shown the reference solution (bold grey line), the order 0 solution (black line) and a solution obtained in the bar with a $E^* = \langle E^0 \rangle$ ('E average', dashed line) for $t = 4.9 \times 10^{-4}$ s as a function of x. As expected, the 'E average' solution is not in phase with the reference solution and shows that this 'natural' filtering is not accurate. On the other hand, the order 0 homogenized solution is already in excellent agreement with the reference solution. On Fig. 3(b) is shown the residual between the order 0 homogenized solution and the reference solution $\hat{u}^0(x, t) - u^\varepsilon(x, t)$. The error amplitude reaches 2 per cent and contains fast variations. On Fig. 3(c) is shown the order 1 residual $\hat{u}^1(x, t) - u^\varepsilon(x, t)$ (bold grey line) and the partial order 2 residual $\hat{u}^{\varepsilon,3/2}(x, t) - u^\varepsilon(x, t)$ (see eq. 52). It can be seen, comparing Figs 3(b) and (c), that the order 1 periodic corrector removes most of the fast variation present in the order 0 residual. The remaining fast variation residual disappears with the partial order 2 residual. The smooth remaining residual is due to the $\langle u^2 \rangle$ that is not computed. In order to check that this smooth remaining residual is indeed an ε^2 residual, this residual computed for $\varepsilon = 0.15$ is overlapped with a residual computed for $\varepsilon = 0.075$ (which corresponds to $l_0 = 3$ mm) to which is applied a factor 4 in amplitude. The fact that these two signals overlap is consistent with a ε^2 residual.

3 NON-PERIODIC CASE

We now give up the hypothesis of periodicity of E^0 and ρ^0 and consider more complex spectra for the size of the heterogeneities. As a specific case, in the following, the bar properties in each cell are now generated randomly around a constant mean value. Homogenization of random structures as studied by Papanicolaou & Varadhan (1979) is not our purpose and the problem is considered as deterministic: the bar properties are completely known and unique for each bar under study. An example of such bar is given in Fig. 4. We still assume a minimum wavelength λ_m (or a maximum wavenumber $k_m = 1/\lambda_m$) for the wavefield u, far enough from the source. It is still reasonable to expect, to some sense, that heterogeneities in the bar, whose size is much smaller than λ_m have a little influence on the wavefield u and that an homogenization procedure can be performed.

3.1 Preliminary: an intuitive solution

The first idea one can have is to consider the whole non-periodic bar as a single periodic cell and apply results obtained in the previous section. The obtained effective medium has a constant density ($\rho^* = \lim_{T \to \infty} \frac{1}{2T} \int_{-T}^{T} \rho^0(x)\mathrm{d}x$) and elastic modulus ($\frac{1}{E^*} = \lim_{T \to \infty} \frac{1}{2T} \int_{-T}^{T} \frac{1}{E^0}(x)\mathrm{d}x$) as shown in Fig. 4 in dashed line. Fig. 5,
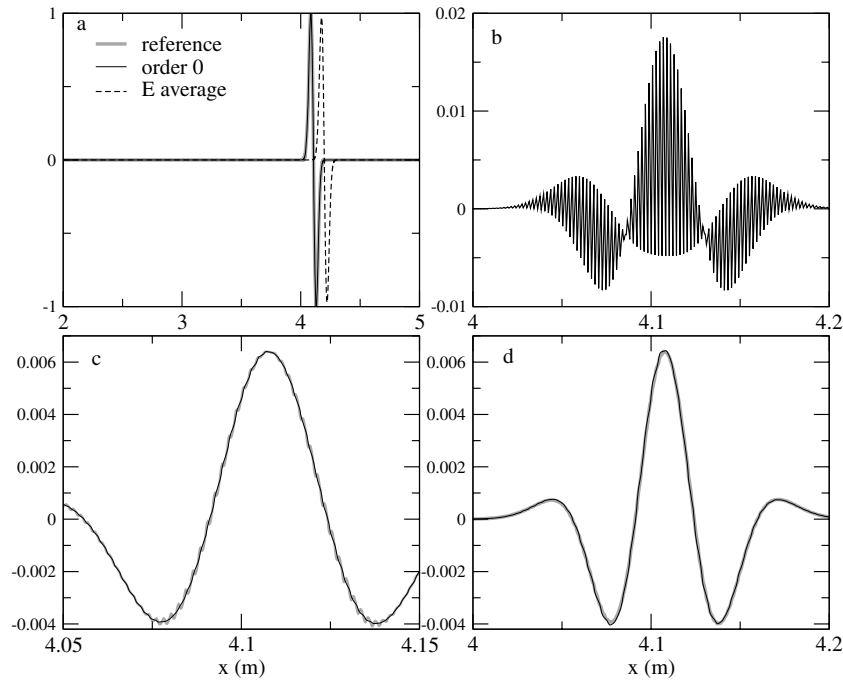
Figure 3. (a) Grey line: displacement $u^\varepsilon(x, t)$ at $t = 4.9 \times 10^{-3}$ s computed in the reference model described Fig. 2. Black line: the order 0 homogenized solution $\hat{u}^0(x, t)$. Dashed line: solution computed in a model obtained by averaging the elastic properties ($\langle\rho^0\rangle$ and $\langle E^0\rangle$). (b) Order 0 residual, $\hat{u}^0(x, t) - u^\varepsilon(x, t)$. (c) Grey line: order 1 residual, $\hat{u}^{\varepsilon,1}(x, t) - u^\varepsilon(x, t)$. Black line: partial order 2 residual, $\hat{u}^{\varepsilon,3/2} - u^\varepsilon(x, t)$ (see eq. 52) (d) Grey line: partial order 2 residual for $\varepsilon = 0.15$. Black line: partial order 2 residual for $\varepsilon = 0.075$ with amplitude multiplied by 4.
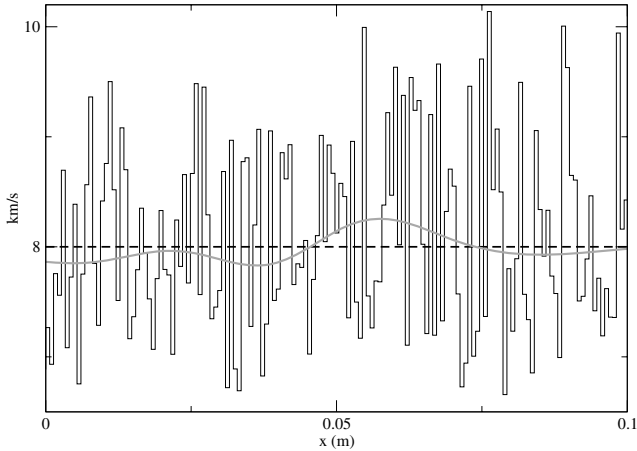

Figure 4. Black line: 10cm sample of the velocity $c = \sqrt{E^0/\rho^0}$ in a non-periodic bar. Dashed line: 'periodic' homogenized velocity if the whole bar is considered has a single periodic cell ($c = \sqrt{\langle E^0\rangle/\langle\rho^0\rangle}$). Grey line: velocity obtained with the spatial filtering ($c = \sqrt{\mathcal{F}^{k_0}(E^0)/\mathcal{F}^{k_0}(\rho^0)}$).

left-hand plot, shows a result obtained in such a medium compared to a reference solution computed in the original bar. The direct arrival is acceptable, but the coda wave corresponding to waves trapped in the heterogeneous medium can not be captured with this simple constant homogenized medium. The waving-hand explanation to that problem is that the wavefield interacts with heterogeneities of the medium whose wavenumbers are as high as k_0 where $k_0 = 1/\lambda_0$ is a wavenumber somewhat larger than the maximum wavenumber of the wavefield, k_m. To be accurate, the effective medium should keep information up to k_0. Without getting

into details, and given k_m, we can indeed distinguish three different propagation regimes (see Aki & Richards 1980), as follows.

● Heterogeneities for which $k_0 \gg k_m$ (scale of the heterogeneities much smaller than the wavelength), where the highly heterogeneous medium can be considered as a homogeneous body with effective elastic properties; this will be the domain of application of the homogenization.
● Heterogeneities for which $k_0 \ll k_m$ (scale of the heterogeneities much larger than the wavelength); the medium then can be considered as a smoothly-varying body.
● Heterogeneities for which $k_0 \approx k_m$. The inhomogeneity scale is comparable to wavelength; this is the domain where coda waves do exist.

The difficulty we are facing, is then to separate these scales correctly in order to homogenize both elastic properties and the wave equation. Remember that this is not so obvious: in the periodic case, the physical quantity to be manipulated, was {not} the elastic constant — but its inverse.

To be able to separate wavenumber above k_0 from that one below k_0, we introduce a mother filter wavelet $w(x)$ (see Fig. 6). w is normalized such that $\int_{\mathbb{R}} w(x)\mathrm{d}x = 1$. When convolved with any function, w acts as a low-pass spatial filter of corner spatial frequency 1. We define $w_{k_0}(x) = k_0 w(xk_0)$ the same but contracted (if $k_0 > 1$) wavelet of corner spatial frequency k_0. We still have $\int_{\mathbb{R}} w_{k_0}(x)dx = 1$. This allows to define a 'filtering operator', for any function $h(x)$

$$\mathcal{F}^{k_0}(h)(x) = \int_{\mathbb{R}} h(x')w_{k_0}(x - x')\mathrm{d}x'. \tag{53}$$

$\mathcal{F}^{k_0}(h)(x)$ is a smooth version of h where all wavenumbers larger than k_0 have been muted to zero. If we apply this filter to $1/E^0$ and
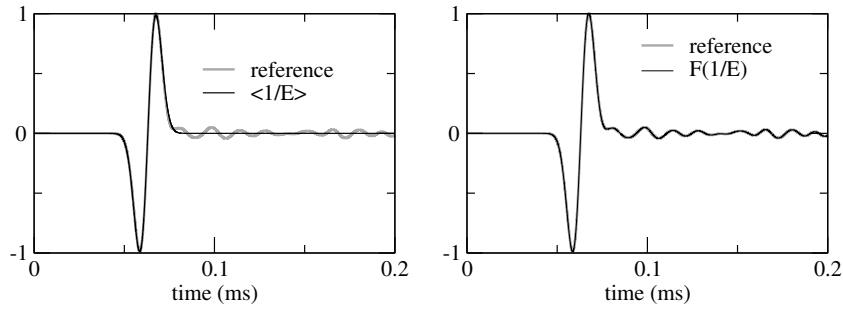
Figure 5. Examples of seismogram computed in bar models presented on Fig. 4. The distance between the source and the receiver is 1 m. The minimum wavelength is 10 cm. Left-hand plot: grey line: reference solution computed in the original bar model; black line: solution obtained in the 'periodic' homogenized model ($\rho^* = \langle \rho^0 \rangle$, $1/E^* = \langle 1/E^0 \rangle$ represented in dashed line Fig. 4). Right-hand plot: grey line: reference solution computed in the original bar model; black line solution obtained by using $1/E^*(x) = \mathcal{F}^{k_0}(1/E^0)$ and $\rho^*(x) = \mathcal{F}^{k_0}(\rho^0)$ as an effective medium (represented in grey line Fig. 4).
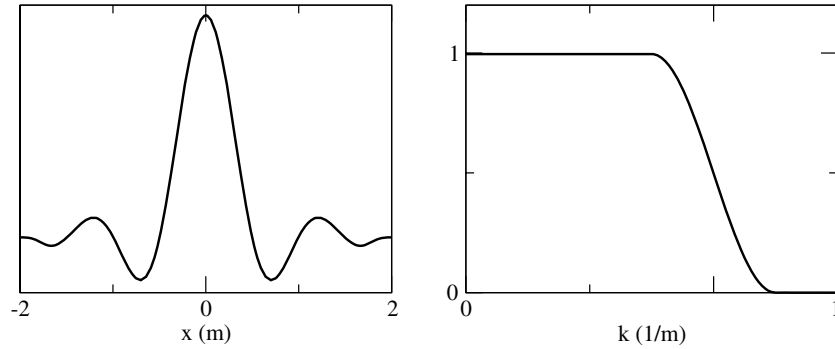

Figure 6. Example of mother filter wavelet $w(x)$ used in practice. On one hand, the cut-off spatial frequency is around 1 but is not sharp and on the other hand, the spatial support can be considered as finite with a good approximation.

ρ^0 and use

$$E^*(x) = \left[\mathcal{F}^{k_0} \left(\frac{1}{E^0} \right) \right]^{-1}(x) \tag{54}$$

and $\rho^*(x) = \mathcal{F}^{k_0}(\rho^0)(x)$ we obtain the smooth medium (Fig. 4, grey line) and the seismogram obtained in such a medium includes the coda waves (Fig. 5, right-hand plot). This intuitive construction of the effective medium seems convenient, but we now need to obtain this result more formally. To do so, one need to construct the sequence of models (E^ε, ρ^ε) and fast parameters [$E(y)$, $\rho(y)$] from (E^0, ρ^0) which is not as straightforward as for the periodic case. Nevertheless, both are necessary to build the homogenization asymptotic expansion. The idea here is to define and keep all the bar properties with wavelength greater than λ_0 and to homogenize all wavelength λ smaller than λ_0 using a spatial filtering similar to (53).

3.2 Set up of the homogenization problem for the non-periodic case

We first introduce the small parameter

$$\varepsilon = \frac{\lambda}{\lambda_m}, \tag{55}$$

where λ is a spatial length or a scale. For the periodic case, λ would be ℓ_0, the periodicity of the model. Because we are not in the periodic case, another parameter is required

$$\varepsilon_0 = \frac{\lambda_0}{\lambda_m}, \tag{56}$$

where λ_0 is the user defined scale below which scales are considered as small scale (microscopic) and above which scales are considered as large scale (macroscopic). While ε is a formal parameter that could be used to show a convergence theorem, ε_0 is a parameter that indicates the degree of smoothness of the homogenized model and accuracy of the homogenized solution (a small ε_0 corresponds to a homogenized model with a lot of details and a precise solution; a large ε_0 corresponds to a smooth homogenized model and an imprecise solution). With that respect, the non-periodic case is different from the periodic case. Indeed, for the periodic case no parameter choice is left to the user, and the accuracy if fixed by the frequency cut-off of the source and the geometry of the elastic structure. For the non-periodic case, we shall see that the introduction of the second small parameters ε_0 allows to specify the accuracy of the solution independently from the geometry of the elastic model. In the following we assume $\varepsilon \leq \varepsilon_0 \ll 1$. As for the periodic case, we work at λ_m fixed. Therefore, a given spatial wavelength λ or wavenumber $k = 1/\lambda$ fully defines $\varepsilon = \lambda/\lambda_m = 1/(k\lambda_m)$. We define $w_m(y) = k_m w(yk_m)$. We assume that w_m support in the space domain is contained in $[-\alpha/k_m, +\alpha/k_m]$ and α is a positive number that depends upon the specific design of w (as w_m has a finite support in the frequency domain, it can not have one in the space domain and $\alpha \to \infty$. Nevertheless, in practice, we assume that w is designed in such a way that the support of w_m can be considered as finite is a good approximation and that a reasonably small α can be found).

Let $Y_x = [x/\varepsilon_0 - \beta/k_m, x/\varepsilon_0 + \beta/k_m]$ be a segment of $\mathbb{R}$ where β is a positive number (much) larger than α. Y_x is the sampling area around x. We define $\mathcal{T} = \{h(x, y) : \mathbb{R}^2 \to \mathbb{R}, 2\beta\lambda_m$-periodic in $y\}$ the set of functions defined in y on Y_0 and extended to $\mathbb{R}$ by

periodicity. We define the filtering operator, for any function $h \in \mathcal{T}$

$$\mathcal{F}(h)(x, y) = \int_{\mathbb{R}} h(x, y') w_m(y - y') \mathrm{d}y' . \tag{57}$$

$\mathcal{F}$ is a linear operator. For a perfectly sharp cut-off low-pass filter in the wavenumber domain, we have, for any h

$$\mathcal{F}[\mathcal{F}(h)] = \mathcal{F}(h) . \tag{58}$$

The last property is not exactly true in practice because, in order to have a compact support for w_m, we do not use a sharp cut-off in the wavenumber domain. We nevertheless assume that (58) is true.

Finally let $\mathcal{V}$, be the set of functions $h(x, y)$ such that, for a given x, the y part of h is periodic and contains only spatial frequencies higher than k_m, plus a constant value in y

$$\mathcal{V} = \{h \in \mathcal{T} / \mathcal{F}(h)(x, y) = \langle h \rangle(x)\} , \tag{59}$$

where

$$\langle h \rangle(x) = \frac{1}{2\beta\lambda_m} \int_{-\beta\lambda_m}^{\beta\lambda_m} h(x, y) \mathrm{d}y , \tag{60}$$

is still the y average of $h(x, y)$ over the periodic cell. In other words, $\mathcal{V}$ is the set of functions that present only fast variations plus a constant value in y. An example of a function h in $\mathcal{V}$ is given in Fig. 7. For any periodic function g with a periodicity smaller than λ_m, choosing β such that an integer number of periodicity fits in Y_0, we have $\mathcal{F}(g) = \langle g \rangle$ and therefore g belongs to $\mathcal{V}$. This implies that the periodic case is a particular case of the following development. As the periodicity has been kept, we still have

$$\forall h \in \mathcal{V}, \ \langle \partial_y h \rangle = 0 , \tag{61}$$

and

$$\forall h \in \mathcal{V}, \ \partial_y h = 0 \Leftrightarrow h(x, y) = \langle h \rangle(x) . \tag{62}$$

It can be shown that, for any function $h \in \mathcal{V}$, its derivative is also in $\mathcal{V}$, and that

$$\forall h \in \mathcal{V} \text{ with } \langle h \rangle = 0 \ \Rightarrow g(x, y) \equiv \int_0^y h(x, y') \mathrm{d}y' \ \in \mathcal{V}. \tag{63}$$

Unfortunately, the product of two functions of $\mathcal{V}$ is not in $\mathcal{V}$ unless these two functions are periodic with the same periodicity smaller than λ_m (and well chosen β as already mentioned).

In this section and the next one, we assume that we have been able to define $[\rho^{\varepsilon_0}(x, y), E^{\varepsilon_0}(x, y)]$ in $\mathcal{T}$ that set up a sequence of parameters

$$\rho^{\varepsilon_0,\varepsilon}(x) \equiv \rho^{\varepsilon_0}\left(x, \frac{x}{\varepsilon}\right) ,$$
$$E^{\varepsilon_0,\varepsilon}(x) \equiv E^{\varepsilon_0}\left(x, \frac{x}{\varepsilon}\right) , \tag{64}$$

and that, with such a set of parameters, a solution to the problem described below exists. This assumption is by far not obvious and the construction of such a $[\rho^{\varepsilon_0}(x, y), E^{\varepsilon_0}(x, y)]$ from $[\rho^0(x), E^0(x)]$, which is the critical point of this paper, is left for Section 3.4.

We look for the solution of the following wave equations

$$\rho^{\varepsilon_0,\varepsilon} \partial_{tt} u^{\varepsilon_0,\varepsilon} - \partial_x \sigma^{\varepsilon_0,\varepsilon} = f ,$$
$$\sigma^{\varepsilon_0,\varepsilon} = E^{\varepsilon_0,\varepsilon} \partial_x u^{\varepsilon_0,\varepsilon} . \tag{65}$$

To solve this problem, the fast space variable y defined (3) is once again used and, in the limit $\varepsilon \to 0$ x and y are treated as independent variables which implies the transformation (4).

The solution to the wave eqs (65) is again sought as an asymptotic expansion in ε, but this time we look for $u^{\varepsilon_0,i}$ and $\sigma^{\varepsilon_0,i}$ in $\mathcal{V}$

$$u^{\varepsilon_0,\varepsilon}(x, t) = \sum_{i=0}^{\infty} \varepsilon^i u^{\varepsilon_0,i}(x, x/\varepsilon, t) = \sum_{i=0}^{\infty} \varepsilon^i u^{\varepsilon_0,i}(x, y, t) ,$$
$$\sigma^{\varepsilon_0,\varepsilon}(x, t) = \sum_{i=-1}^{\infty} \varepsilon^i \sigma^{\varepsilon_0,i}(x, x/\varepsilon, t) = \sum_{i=-1}^{\infty} \varepsilon^i \sigma^{\varepsilon_0,i}(x, y, t) . \tag{66}$$

Note that imposing $u^{\varepsilon_0,i}$ and $\sigma^{\varepsilon_0,i}$ in $\mathcal{V}$ is a strong condition that mainly means that only slow variations must appear in x and only fast in y. Introducing expansions (66) in the wave eqs (65) and using (4) we obtain

$$\rho^{\varepsilon_0} \partial_{tt} u^{\varepsilon_0,i} - \partial_x \sigma^{\varepsilon_0,i} - \partial_y \sigma^{\varepsilon_0,i+1} = f\delta_{i,0} , \tag{67}$$
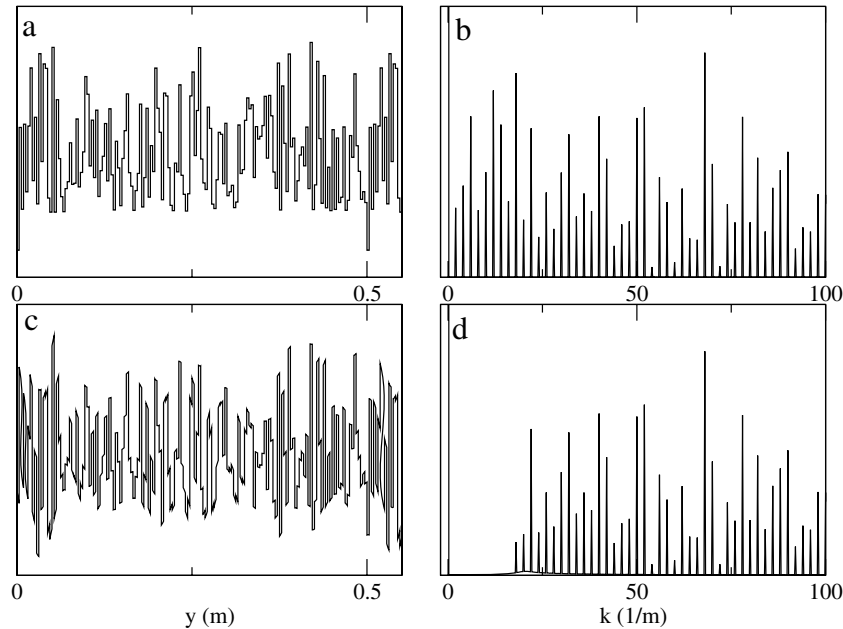

Figure 7. Example of a function $h(x, y) \in \mathcal{T}$ but not in $\mathcal{V}$ (graph a) and $h(x, y) \in \mathcal{V}$ (graph c) for a $k_m = 16\,\mathrm{m}^{-1}$ plotted for a given x as a function of y and their respective power spectra (graphs b and d) for positive wavenumber (k). It can be seen that, for $h(x, y) \in \mathcal{V}$ the power spectrum is 0 is the range $[0\,\mathrm{m}^{-1}, 16\,\mathrm{m}^{-1}]$. Both functions are periodic with a periodicity of 0.5 m.

$$\sigma^{\varepsilon_0,i} = E^{\varepsilon_0} \left(\partial_x u^{\varepsilon_0,i} + \partial_y u^{\varepsilon_0,i+1} \right), \tag{68}$$

which need to be solved for each $i \geq -2$ and $i \geq -1$, respectively.

3.3 Resolution of the homogenization problem

We follow the same procedure as for the periodic case. We work at ε_0 fixed and, to ease the notations, the ε_0 superscript is only kept for the bar properties and correctors, but dropped for $u^{\varepsilon_0,i}, \sigma^{\varepsilon_0,i}$. Because the y periodicity is kept in $\mathcal{V}$, the resolution of the homogenized equations is almost the same as in the periodic case.

- As for the periodic case, eqs (67) for $i = -2$ and (68) for $i = -1$ gives $\sigma^{-1} = 0$ and $u^0 = \langle u^0 \rangle$.
- Eqs (67) for $i = -1$ and (68) for $i = 0$ implies $\sigma^0 = \langle \sigma^0 \rangle$ and

$$\partial_y \left(E^{\varepsilon_0} \partial_y u^1 \right) = -\partial_y E^{\varepsilon_0} \, \partial_x u^0. \tag{69}$$

Using the linearity of the last equation we can separate the variables and look for a solution of the form

$$u^1(x, y) = \chi^{\varepsilon_0,1}(x, y)\partial_x u^0(x) + \langle u^1 \rangle(x). \tag{70}$$

As $u^1 \in \mathcal{V}$ and $u^0 = \langle u^0 \rangle$, $\chi^{\varepsilon_0,1}$ must lie in $\mathcal{V}$ and satisfies

$$\partial_y \left[E^{\varepsilon_0} \left(1 + \partial_y \chi^{\varepsilon_0,1} \right) \right] = 0, \tag{71}$$

with periodic boundary conditions. We impose $\langle \chi^{\varepsilon_0,1} \rangle(x) = 0$. A solution in $\mathcal{V}$ to the last equation exists only if E^{ε_0} have been correctly build, that is, using the general solution (22), $1/E^{\varepsilon_0}$ must lie in $\mathcal{V}$. If this condition is met, $\chi^{\varepsilon_0,1}(x, y)$ is in $\mathcal{V}$ and

$$\partial_y \chi^{\varepsilon_0,1}(x, y) = -1 + \left\langle \frac{1}{E^{\varepsilon_0}} \right\rangle^{-1}(x) \; \frac{1}{E^{\varepsilon_0}(x, y)}. \tag{72}$$

As for the periodic case, we find the order 0 constitutive relation

$$\sigma^0(x) = E^{\varepsilon_0 *}(x)\partial_x u^0(x), \tag{73}$$

with

$$E^{\varepsilon_0 *}(x) = \left\langle E^{\varepsilon_0} \left(1 + \partial_y \chi^{\varepsilon_0,1} \right) \right\rangle(x), \tag{74}$$

$$= \left\langle \frac{1}{E^{\varepsilon_0}} \right\rangle^{-1}(x). \tag{75}$$

- Eqs (67) for $i = 0$ and (68) for $i = 1$ give

$$\rho^{\varepsilon_0} \partial_{tt} u^0 - \partial_x \sigma^0 - \partial_y \sigma^1 = f, \tag{76}$$

$$\sigma^1 = E^{\varepsilon_0} \left(\partial_y u^2 + \partial_x u^1 \right). \tag{77}$$

To be able to obtain σ^1 in $\mathcal{V}$, (76) implies that ρ^{ε_0} must lie in $\mathcal{V}$. Taking the average on (76) together with (73) allows to find the order 0 wave equation

$$\langle \rho^{\varepsilon_0} \rangle \partial_{tt} u^0 - \partial_x \sigma^0 = f \tag{78}$$

$$\sigma^0 = E^{\varepsilon_0 *}\partial_x u^0. \tag{79}$$

Subtracting (78) from (76), together with (77) gives

$$\partial_y \left(E^{\varepsilon_0} \partial_y u^2 \right) = -\partial_y E^{\varepsilon_0} \, \partial_x \langle u^1 \rangle - \partial_y \left(E^{\varepsilon_0} \chi^{\varepsilon_0,1} \right) \partial_{xx} u^0$$
$$- \partial_y \left(E^{\varepsilon_0} \partial_x \chi^{\varepsilon_0,1} \right) \partial_x u^0 + (\rho^{\varepsilon_0} - \langle \rho^{\varepsilon_0} \rangle)\partial_{tt} u^0. \tag{80}$$

We can once again use the linearity of the last equation and we can separate the variables and look for a solution of the form

$$u^2(x, y) = \chi^{\varepsilon_0,2}(x, y)\partial_{xx} u^0(x) + \chi^{\varepsilon_0,2x}(x, y)\partial_x u^0(x)$$
$$+ \chi^{\varepsilon_0,1}(x, y)\partial_x \langle u^1 \rangle(x) + \chi^{\varepsilon_0,\rho}(x, y)\partial_{tt} u^0 + \langle u^2 \rangle(x), \tag{81}$$

where $\chi^{\varepsilon_0,2}$, $\chi^{\varepsilon_0,2x}$ and $\chi^{\varepsilon_0,\rho}$ are solutions of

$$\partial_y \left[E^{\varepsilon_0} \left(\chi^{\varepsilon_0,1} + \partial_y \chi^{\varepsilon_0,2} \right) \right] = 0, \tag{82}$$

$$\partial_y \left[E^{\varepsilon_0} \left(\partial_x \chi^{\varepsilon_0,1} + \partial_y \chi^{\varepsilon_0,2x} \right) \right] = 0, \tag{83}$$

$$\partial_y \left[E^{\varepsilon_0} \partial_y \chi^{\varepsilon_0,\rho} \right] = \rho^{\varepsilon_0} - \langle \rho^{\varepsilon_0} \rangle, \tag{84}$$

with $\chi^{\varepsilon_0,2}$, $\chi^{\varepsilon_0,2x}$ and $\chi^{\varepsilon_0,\rho}$ in $\mathcal{V}$ and $\langle \chi^{\varepsilon_0,2} \rangle = \langle \chi^{\varepsilon_0,2x} \rangle = \langle \chi^{\varepsilon_0,\rho} \rangle = 0$. An important point here is to check that it exists a solution to (82) in $\mathcal{V}$. The general solution of (82) is

$$\chi^{\varepsilon_0,2}(x, y) = a \int_0^y \frac{1}{E^{\varepsilon_0}}(x, y')\mathrm{d}y' - \int_0^y \chi^{\varepsilon_0,1}(x, y')\mathrm{d}y' + b. \tag{85}$$

The periodic condition and $\langle \chi^{\varepsilon_0,1} \rangle = 0$ give $a = 0$. We therefore have $\chi^{\varepsilon_0,2} = -\int_0^y \chi^{\varepsilon_0,1}(x, y')\mathrm{d}y' + b$ and, thanks to (63), $\chi^{\varepsilon_0,2}$ is indeed in $\mathcal{V}$. Similarly, it can be shown that $\chi^{\varepsilon_0,2x}$ is in $\mathcal{V}$. On the other hand, in general, $\chi^{\varepsilon_0,\rho}$ is not in $\mathcal{V}$ as the product of two functions in $\mathcal{V}$ is not in $\mathcal{V}$. Nevertheless, in the periodic case with a periodicity smaller than $1/k_0$, the product of two functions are still periodic with the same periodicity and therefore belongs to $\mathcal{V}$. In that case, $\chi^{\varepsilon_0,\rho}$ is indeed in $\mathcal{V}$.

Introducing (81) into (77) and taking the average, we find the order 1 constitutive relation

$$\langle \sigma^1 \rangle = E^{\varepsilon_0 *}\partial_x \langle u^1 \rangle + E^{\varepsilon_0,1x*}\partial_x u^0 + E^{\varepsilon_0,1*}\partial_{xx} u^0 + E^{\varepsilon_0,\rho *}\partial_{tt} u^0 \tag{86}$$

with

$$E^{\varepsilon_0,1*} = \left\langle E^{\varepsilon_0} \left(\chi^{\varepsilon_0,1} + \partial_y \chi^{\varepsilon_0,2} \right) \right\rangle, \tag{87}$$

$$E^{\varepsilon_0,1x*} = \left\langle E^{\varepsilon_0} \left(\partial_x \chi^{\varepsilon_0,1} + \partial_y \chi^{\varepsilon_0,2x} \right) \right\rangle, \tag{88}$$

$$E^{\varepsilon_0,\rho *} = \left\langle E^{\varepsilon_0} \partial_y \chi^{\varepsilon_0,\rho} \right\rangle. \tag{89}$$

As we have already seen, $\chi^{\varepsilon_0,2}$ in $\mathcal{V}$ and $\langle \chi^{\varepsilon_0,2} \rangle = 0$ impose $\partial_y \chi^{\varepsilon_0,2} = -\chi^{\varepsilon_0,1}$ and therefore $E^{\varepsilon_0,1*} = 0$. Similarly, we have $E^{\varepsilon_0,1x*} = 0$.

Finally, using (70) and taking the average of eqs (67) for $i = 1$ gives the order 1 wave equation

$$\langle \rho^{\varepsilon_0} \rangle \partial_{tt} \langle u^1 \rangle + \langle \rho^{\varepsilon_0} \chi^{\varepsilon_0,1} \rangle \partial_x \partial_{tt} u^0 - \partial_x \langle \sigma^1 \rangle = 0$$
$$\langle \sigma^1 \rangle = E^{\varepsilon_0 *}\partial_x \langle u^1 \rangle + E^{\rho,\varepsilon_0 *}\partial_{tt} u^0. \tag{90}$$

In general, $\rho^{\varepsilon_0} \chi^{\varepsilon_0,1}$ is not in $\mathcal{V}$, but we still have $E^{\rho,\varepsilon_0 *} = \langle \rho^{\varepsilon_0} \chi^{\varepsilon_0,1} \rangle$ and similarly to the periodic case, the last equation can be rewritten as

$$(\langle \rho^{\varepsilon_0} \rangle + \partial_x E^{\rho,\varepsilon_0 *})\partial_{tt} u^1 - \partial_x \langle \tilde{\sigma}^1 \rangle = 0$$
$$\langle \tilde{\sigma}^1 \rangle = E^{\varepsilon_0 *}\partial_x \langle u^1 \rangle, \tag{91}$$

where $\langle \tilde{\sigma}^1 \rangle = \langle \sigma^1 \rangle - E^{\rho,\varepsilon_0 *}\partial_{tt} u^0$.

As we have seen earlier, in general $\rho^{\varepsilon_0} \chi^{\varepsilon_0,1}$ and $\chi^{\varepsilon_0,\rho}$ are not in $\mathcal{V}$ which means that, in general, the whole non-periodic development presented is only valid for the order 0 and the first order corrector. It is valid for higher order only if ρ^{ε_0} has no fast variation or for periodic variations. Nevertheless, in practice, $\chi^{\varepsilon_0,\rho}$ and $\rho^{\varepsilon_0} \chi^{\varepsilon_0,1}$ are very close to be in $\mathcal{V}$ and the whole development can be used as we will see in the non-periodic example.

As for the periodic case, the different orders can be combined as shown in Section 2.3.

3.4 Construction of E^{ε_0} and ρ^{ε_0}

We present here two ways of building E^{ε_0} and ρ^{ε_0} in $\mathcal{T}$ with the following constraints obtained in the previous sections:

(i) ρ^{ε_0} and χ^{ε_0} must lie in $\mathcal{V}$ (see eqs 76 and 72).
(ii) ρ^{ε_0} and E^{ε_0} must be positive functions.
(iii) $\rho^{\varepsilon_0}(x, x/\varepsilon_0) = \rho^0(x)$ and $E^{\varepsilon_0}(x, x/\varepsilon_0) = E^0(x)$.

The first constraint is necessary to obtain solutions in $\mathcal{V}$ at least up to the order 1.

3.4.1 Direct construction

The 1-D case is interesting because it gives an explicit formula for χ^{ε_0}, and implies that $1/E^{\varepsilon_0}$ should be in $\mathcal{V}$ (constraint (i)) so that a solution to the non-periodic homogenized problem exists. Thanks to this explicit constraint, we can propose, for a given x and any $y \in Y_x$,

$$\rho^{\varepsilon_0}(x, y) = \mathcal{F}^{k_0}(\rho^0)(x) + [\rho^0 - \mathcal{F}^{k_0}(\rho^0)](\varepsilon_0 y), \tag{92}$$

$$E^{\varepsilon_0}(x, y) = \left\{ \mathcal{F}^{k_0}\left(\frac{1}{E^0}\right)(x) + \left[\frac{1}{E^0} - \mathcal{F}^{k_0}\left(\frac{1}{E^0}\right)\right](\varepsilon_0 y)\right\}^{-1}, \tag{93}$$

and then extended to $\mathbb{R}$ in y by periodicity. ρ^{ε_0} and E^{ε_0} are by construction in $\mathcal{T}$. Thanks to the fact that, for any h

$$\mathcal{F}^{k_0}\left(\mathcal{F}^{k_0}(h)\right) = \mathcal{F}^{k_0}(h), \tag{94}$$

it can be checked that ρ^{ε_0} and $1/E^{\varepsilon_0}$ are in $\mathcal{V}$ (which is not the case of E^{ε_0}). Note that this is not completely true in practice because the filter w has not a sharp cut-off, which implies that (94) is not fully accurate. We consider this side effect as being negligible. We define

$$\rho^{\varepsilon_0,\varepsilon}(x) = \rho^{\varepsilon_0}\left(x, \frac{x}{\varepsilon}\right), \tag{95}$$

$$E^{\varepsilon_0,\varepsilon}(x) = E^{\varepsilon_0}\left(x, \frac{x}{\varepsilon}\right), \tag{96}$$

and one can check that $\rho^{\varepsilon_0,\varepsilon_0} = \rho^0$ and $E^{\varepsilon_0,\varepsilon_0} = E^0$.

For most standard applications, ρ^{ε_0} and E^{ε_0} are positive functions for any filter wavelet w. Nevertheless, for some extreme cases (e.g. a single discontinuity with several orders of magnitude of elastic modulus contrast), some filter wavelet w designs could lead to a negative E^{ε_0}. In such an extreme case, on should make sure that the design of w allows ρ^{ε_0} and E^{ε_0} to be positive functions.

Finally, we can check that

$$\frac{1}{E^{\varepsilon_0,*}} = \left\langle \frac{1}{E^{\varepsilon_0}} \right\rangle = \mathcal{F}^{k_0}\left(\frac{1}{E^0}\right)(x), \tag{97}$$

which is the intuitive effective elastic modulus (54) guessed in Section 3.1.

3.4.2 Implicit construction

For higher dimensions than 1-D, a cell problem, similar to (71), arises (see, for example Sanchez-Palencia 1980). Unfortunately, in general, there is no explicit solution to this cell problem leading to an analytical solution equivalent to (72) (there is one for layered media,

but it can be considered as a 1-D case). The direct solution explained above to build E^{ε_0} is therefore not available for higher dimensions (it still is for ρ^{ε_0}). We propose here a procedure that gives a similar result as the explicit construction without the knowledge that the construction should to be done on $1/E^0$. The main interest of the procedure is it can be generalized to a higher space dimension. It is based on the work of Papanicolaou & Varadhan (1979) on the homogenization for random media. They suggest to work with the gradient of correctors rather than to work on corrector directly. If we name

$$G^{\varepsilon_0} = \partial_y \chi^{\varepsilon_0,1} + 1, \tag{98}$$

$$H^{\varepsilon_0}(x, y) = E^{\varepsilon_0}(x, y)G^{\varepsilon_0}(x, y), \tag{99}$$

a solution to our problem in $\mathcal{V}$ up to the order 1 is found if we can build $E^{\varepsilon_0}(x, y)$ such that $(H^{\varepsilon_0}, G^{\varepsilon_0}) \in \mathcal{V}$ and $\langle G^{\varepsilon_0} \rangle = 1$.

To do so, we propose the following procedure:

(i) Build a start $E_s^{\varepsilon_0}$ defined as, for a given x and for any $y \in Y_x$, $E_s^{\varepsilon_0}(x, y) = E^0(\varepsilon_0 y)$ and then extended to $\mathbb{R}$ in y by periodicity ($E_s^{\varepsilon_0}$ is therefore in $\mathcal{T}$). Then solve (71) with periodic boundary conditions on Y_x to find $\chi_s^{\varepsilon_0,1}(x, y)$.

(ii) Compute $G_s^{\varepsilon_0} = \partial_y \chi_s^{\varepsilon_0,1} + 1$, then $H_s^{\varepsilon_0}(x, y) = E_s^{\varepsilon_0}(x, y)G_s^{\varepsilon_0}(x, y)$ and finally

$$G^{\varepsilon_0}(x, y) = \frac{1}{\mathcal{F}\left(G_s^{\varepsilon_0}\right)(x, x/\varepsilon_0)}\left(G_s^{\varepsilon_0} - \mathcal{F}\left(G_s^{\varepsilon_0}\right)\right)(x, y) + 1, \tag{100}$$

$$H^{\varepsilon_0}(x, y) = \frac{1}{\mathcal{F}\left(G_s^{\varepsilon_0}\right)(x, x/\varepsilon_0)} \times \left[\left(H_s^{\varepsilon_0} - \mathcal{F}\left(H_s^{\varepsilon_0}\right)\right)(x, y) + \mathcal{F}\left(H_s^{\varepsilon_0}\right)(x, x/\varepsilon_0)\right]. \tag{101}$$

At this stage, we have $(H^{\varepsilon_0}, G^{\varepsilon_0}) \in \mathcal{V}^2$ and $\langle G^{\varepsilon_0} \rangle = 1$.

(iii) From (99) and (74), we have

$$E^{\varepsilon_0}(x, y) = \frac{H_s^{\varepsilon_0}}{G_s^{\varepsilon_0}}(x, y), \tag{102}$$

$$E^{*,\varepsilon_0}(x) = \langle H^{\varepsilon_0} \rangle(x) = \frac{\mathcal{F}\left(H_s^{\varepsilon_0}\right)}{\mathcal{F}\left(G_s^{\varepsilon_0}\right)}(x, x/\varepsilon_0). \tag{103}$$

(iv) Once $E^{\varepsilon_0}(x, y)$ is known, follow the whole homogenization procedure to find the different correctors can be pursued.

Once again, we insist on the fact that the main interest of this procedure is that obtaining an explicit solution to the cell problem is not required and it can be extended to 2-D or 3-D.

Remarks

• In practical cases, the bar is finite and Y_x can be chosen to enclose the whole bar. In that case, the dependence to the macroscopic location x in $\chi_s^{\varepsilon_0,1}$, $G_s^{\varepsilon_0}$, $H_s^{\varepsilon_0}$ and $E_s^{\varepsilon_0}$ disappears.

• The step (i) of the implicit construction procedure involves to solve (71) with periodic boundary conditions on Y_x. This step implies the use of a finite element solver on a single large domain (if Y_0 is set as the whole bar) or on a set of smaller domains (Y_x) and this implies that a mesh, or a set of meshes, of the elastic properties in the Y_x domain must be designed. Therefore, even if the meshing problem for the elastic wave propagation in order 0 homogenized model is much simpler for the than for the original model, the problem is still not mesh free. Fine meshes still must be

designed to solve the homogenization problem. Nevertheless, these meshes can be based on tetrahedra even if the wave equation solver is based on hexahedra. Moreover, as the homogenization problem is time independent, the consequences of very small or badly shaped elements on the computing time are limited.

We can check that this procedure gives a correct result on our 1-D case.

(i) Taking Y_x as $\mathbb{R}$ (β infinite), the first step allows to find $\partial_y \chi_s^{\varepsilon_0,1}(y) = \frac{C}{E^0}(\varepsilon_0 y) - 1$ where $C = (\lim_{T\to\infty} \frac{1}{2T} \int_{-T}^{T} \frac{1}{E^0}(x)\mathrm{d}x)^{-1}$.

(ii) H^{ε_0} and G^{ε_0} are straight forward to compute from step (i). We have

$$G^{\varepsilon_0}(x,y) = \frac{1}{\mathcal{F}^{k_0}\left(\frac{1}{E^0}\right)}(x)\left[\frac{1}{E^0} - \mathcal{F}^{k_0}\left(\frac{1}{E^0}\right)\right](\varepsilon_0 y) + 1, \quad (104)$$

where the fact that, for any h, $\mathcal{F}(h)(x/\varepsilon_0) = \mathcal{F}^{k_0}(h)(x)$. We also find $H^{\varepsilon_0}(x,y) = [\mathcal{F}^{k_0}(\frac{1}{E^0})(x)]^{-1}$.

(iii) The third step allows to find

$$E^{\varepsilon_0}(x,y) = \left\{\left[\frac{1}{E^0} - \mathcal{F}^{k_0}\left(\frac{1}{E^0}\right)\right](\varepsilon_0 y) + \mathcal{F}^{k_0}\left(\frac{1}{E^0}\right)(x)\right\}^{-1} \quad (105)$$

$$E^{*,\varepsilon_0}(x) = \left[\mathcal{F}^{k_0}\left(\frac{1}{E^0}\right)(x)\right]^{-1} \quad (106)$$

which are the desired results.

3.5 Convergence of the asymptotic solution with ε_0

As for this non-periodic case, we have built a classical periodic homogenization scheme, the convergence theorem is still valid: $u^{\varepsilon_0,\varepsilon}$ converges in the appropriate sense to the leading order asymptotic term $u^{\varepsilon_0,i=0}$ as ε tends towards 0 (see Section 2.1). In the periodic case, one particular ε ($\varepsilon = \ell_0/\lambda_m$) corresponds to the 'real' case we wish to approximate. In the non-periodic case, it is $\varepsilon = \varepsilon_0$, but this is true for any ε_0. Let us name u^{ref} the reference solution obtained in the 'real model' (ρ^0, E^0). Thanks to the condition (iii) of Section 3.4, we have, for all ε_0, $u^{ref} = u^{\varepsilon_0,\varepsilon_0}$. Therefore, still using the classical convergence theorem, we know that the leading order asymptotic term $u^{\varepsilon_0,0}$ will converge towards u^{ref} as ε_0 tends towards 0. Furthermore, using (47), we also have

$$\hat{u}^{\varepsilon_0,1} = u^{ref} + O\left(\varepsilon_0^2\right). \quad (107)$$

3.6 A numerical experiment for a non-periodic case

As mentioned above, the only case that can be considered practically is $\varepsilon = \varepsilon_0$. A consequence of this is, in order to check the convergence with ε, the only way is to vary ε_0 through the filter w_{k_0} used to separate the scales.

As for the periodic case, we perform a numerical experiment using SEM. We generate a bar model composed of slices of 0.64 mm thick in which the properties E and ρ are constant and determined randomly. A sample of the E^0 values are shown on Fig. 8. We first build $E^{\varepsilon_0}(x,y)$ and $\rho^{\varepsilon_0}(x,y)$ using one of the two methods described in Section 3.4 (they both give the same result). Two examples of homogenized E^{*,ε_0} can be seen on Fig. 8. Then the cells problem (71), (82), (83) and (84) are solved for each x of the SEM mesh using the same finite elements method than the one used for
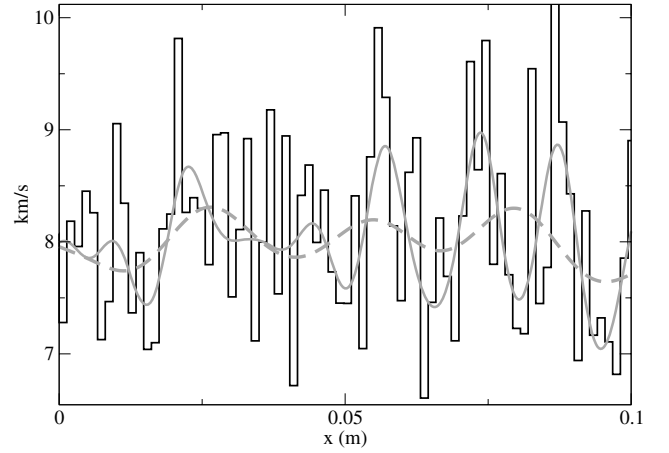
Figure 8. Sample (10 cm) of the bar velocity (black line, km s^{-1}) and two examples of order 0 homogenized velocities (bold grey line for $\varepsilon_0 = 0.125$ and bold dashed grey line for $\varepsilon_0 = 0.25$). The density has a similar but uncorrelated pattern.

the periodic case. This part is more time consuming than for the periodic case because these equations have to be solved on many large Y_x segments or on a single global Y_0 segment. The wave equation

$$\tilde{\rho}\partial_{tt}u - \partial_x\left(E^{\varepsilon_0,*}\partial_x u\right) = f, \quad (108)$$

where $\tilde{\rho} = \langle\rho^{\varepsilon_0}\rangle + \varepsilon_0\partial_x E^{\rho,\varepsilon_0*}$, $u = \langle\hat{u}^{\varepsilon_0,1}\rangle$ and $f = \hat{f}^{\varepsilon_0,1}$, is then solved using the SEM.

The source is the same as for the periodic case as well as the set up of the SEM. In the case presented here, $\varepsilon_0 \simeq 0.125$. Once the simulation is done, for a given time step corresponding to $t = 4.9 \times 10^{-4}$ s, the complete order 1 solution can be computed with (46). We can also compute the incomplete order 2 solution

$$\hat{u}^{\varepsilon_0,3/2} = \left[1 + \varepsilon_0\chi^{\varepsilon_0,1}\left(x,\frac{x}{\varepsilon_0}\right)\partial_x + \varepsilon_0^2\left(\chi^{\varepsilon_0,2x}\left(x,\frac{x}{\varepsilon_0}\right)\partial_x\right.\right.$$
$$\left.\left. + \chi^{\varepsilon_0,2}\left(x,\frac{x}{\varepsilon_0}\right)\partial_{xx} + \chi^{\varepsilon_0,\rho}\left(x,\frac{x}{\varepsilon_0}\right)\partial_{tt}\right)\right]\langle\hat{u}^{\varepsilon_0,1}\rangle. \quad (109)$$

On Fig. 9 are shown the results of the simulation. On the upper left plot (Fig. 9a) are shown the reference solution (bold grey line), the order 0 solution (black line) and a solution obtained in bar with an effective $E^* = \mathcal{F}^{k_0}(E^0)$ ('E average', dashed line) for $t = 4.9 \times 10^{-4}$ s as a function of x. Note the strong coda wave trapped in the random model on the left of the ballistic pulse which was not at all present in the periodic case. As expected, the 'E average' solution is not in phase with the reference solution and shows that this 'natural' filtering is not accurate. On the other hand, the order 0 homogenized solution is already in excellent agreement with the reference solution. On Fig. 9(b) is shown the residual between the order 0 homogenized solution and the reference solution $\hat{u}^{\varepsilon_0,0}(x,t) - u^{ref}(x,t)$. The error amplitude reaches 1 per cent and contains fast variations. On Fig. 9(c) is shown the order 1 residual $\hat{u}^{\varepsilon_0,1}(x,t) - u^{ref}(x,t)$ (bold grey line) and the partial order 2 residual $\hat{u}^{\varepsilon_0,3/2}(x,t) - u^{ref}(x,t)$ (see eq. 109). It can be seen comparing Figs 9(b) and (c) that the order 1 periodic corrector removes most of the fast variation present in the order 0 residual. The remaining fast variation residual disappears with the partial order 2 residual. The smooth remaining residual is due to the $\langle u^2\rangle$ that is not computed. In order to check that this smooth remaining residual is indeed an ε^2_0 residual, the same residual, computed for $\varepsilon_0 = 0.125$ is compared to the partial order 2 residual computed for $\varepsilon_0 = 0.0625$ (multiplying its amplitude by 4) and for $\varepsilon_0 = 0.25$ (dividing its amplitude by 4).
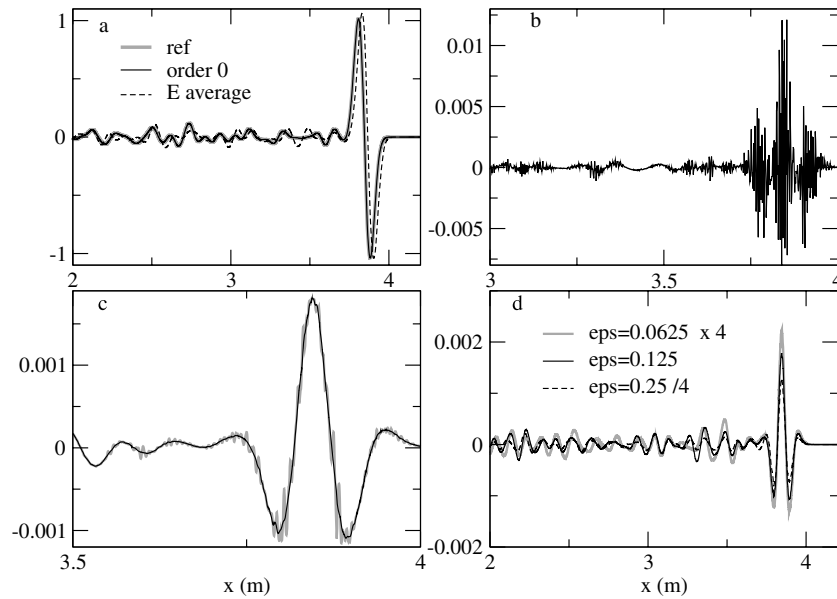
Figure 9. (a) Grey line: displacement $u^{ref}(x, t)$ at $t = 4.9 \times 10^{-3}$ s computed in the reference model described Fig. 2. Black line: the order 0 homogenized solution $\hat{u}^0(x, t)$. Dashed line: solution computed in a model obtained by averaging the elastic properties $[\mathcal{F}^{k_0}(\rho^0)$ and $\mathcal{F}^{k_0}(E^0)]$. (b) Order 0 residual, $\hat{u}^0(x, t) - u^{ref}(x, t)$. (c) Grey line: order 1 residual, $\hat{u}^{\varepsilon_0,1}(x, t) - u^{ref}(x, t)$. Black line: partial order 2 residual, $\hat{u}^{\varepsilon_0,3/2} - u^{ref}(x, t)$ (see eq. 109). (d) Black line: partial order 2 residual for $\varepsilon_0 = 0.125$ mm. Grey line: partial order 2 residual for $\varepsilon_0 = 0.0625$ mm with amplitude multiplied by 4. Dashed line: partial order 2 residual for $\varepsilon_0 = 0.25$ mm with amplitude divided by 4.

It can be seen that these three signals overlap but not completely. This is consistent with a $\varepsilon^2{}_0$ residual but it shows that the approximations made, mainly on the fact that support of the filters w_{k_0} has been truncated to make their support finite, has some effect on the convergence rate.

4 CONCLUSIONS AND PERSPECTIVES

We have presented an extension of the classical two scale homogenization from 1-D periodic media to 1-D non-periodic media. This extension does not hold beyond the order 1, but for the periodic case. This non-periodic homogenization procedure is based on the introduction of a spatial filter, that allows to separate scales in the heterogeneity pattern of the medium. In the wavenumber domain, the location of the filter cut-off k_0 that separates slow and fast variations in the physical properties, is left at the discretion of the user, but must be chosen such that k_0 is larger than the maximum wavenumber of the wavefield k_m to obtain an accurate result. For the leading order of this asymptotic theory, the wavefield computed in the homogenized medium converge towards the reference solution as $\varepsilon_0 = k_m/k_0$. The level of accuracy can therefore be chosen by selecting the appropriate k_0.

In contrast to the periodic case, the general solution presented is computationally intensive. Indeed, the non-periodic homogenization requires to solve the so-called cell problem (eq. 71) over the full model (in one time or in a multitude of smaller problems) and not on a single cell as in the periodic case; and this can be very challenging. Nevertheless, this cell problem is time-independent, and has to be solved only once for the whole medium (using a classical finite element method); and simulating wave propagation with SEM, in the smooth, homogenized medium is much less time-consuming, than doing the same in the rough, initial one.

Another issue is that the effective medium resulting from the homogenization procedure at the leading order, is often oscillating in space. These oscillations result from the application of the spatial filter to discontinuities. Because the spatial cut-off k_0 is chosen larger than the maximum wavenumber k_m, the spatial oscillations of the medium may be faster than the maximum ones of the wavefield. For the SEM point of view, this must be taken into account and the classical rule used to sample the wavefield (e.g. 2 minimum wavelength per degree 8 elements) for piecewise content medium does not fully apply. The solution is just to increase the number of elements per wavelength, but this unfortunately has a numerical cost. The optimum sampling of the wavefield in such a case remains to be studied.

A critical aspect of this work is that the methodology exposed for the 1-D case can be extended to higher dimensions because it is not based on the knowledge of an analytical solution of the cell problem as it was the case in Capdeville & Marigo (2007). An important perspective of this work is then to extend it to 2- and 3-D. This should allow to solve many meshes difficulties that arise when using the SEM for wave propagation simulation in complex 3-D media.

Finally, we underline the fact that the results obtained may have important applications in inverse problems for the Earth structure: first it is shown how to define a multiscale parametrization depending on the wavefield properties; second, physical quantities that should be inverted for (here $1/E$), directly appear in the set of equations involved in the homogenization procedure. Moreover, the periodic correctors should allow to make inferences about local effect at source and receiver locations.

A patent (Capdeville 2009) has been filed on the non-periodic homogenization process by the 'Centre national de la recherche scientifique' (CNRS) (this is by no mean a restriction to any academic research on the subject).

reviewer for their constructive remarks. This work was supported by the ANR MUSE under the blanc programme.

REFERENCES

Abdelmoula, R. & Marigo, J.-J., 2000. The effective behavior of a fiber bridged crack, *J. Mech. Phys. Solids,* **48**(11), 2419–2444.

Aki, K. & Richards, P., 1980. *Quantitative Seismology: Theory and Methods,* Freeman, San Francisco.

Allaire, G., 1992. Homogenization and two-scale convergence. *SIAM J. Math. Anal.,* **23**, 1482–1518.

Allaire, G. & Conca, C., 1998. Boundary layers in the homogenization of a spectral problem in fluid–solid structures, *SIAM J. Math. Anal.,* **29**(2), 343–379.

Allaire, G., Palombaro, M. & Rauch, J., 2009. Diffractive behavior of the wave equation in periodic media: weak convergence analysis, *Annali di Matematica,* **188**, 561–589.

Auriault, J. & Bonnet, G., 1985. Dynamique des composites élastiques périodiques, *Arch. Mech.* **37**(4–5), 269–284.

Auriault, J.-L. & Sanchez-Palencia, E., 1977. Étude du comportement macroscopique d'un milieu poreux saturé déformable, *J. Mécanique,* **16**(4), 575–603.

Backus, G., 1962. Long-wave elastic anisotropy produced by horizontal layering, *j. geophys. Res.,* **67**(11), 4427–4440.

Bensoussan, A., Lions, J.-L. & Papanicolaou, G., 1978, *Asymptotic Analysis of Periodic Structures,* North Holland, Amsterdam.

Briane, M., 1994. Homogenization of a nonperiodic material, *J. Math. Pures Appl. (9),* **73**(1), 47–66.

Capdeville, Y., 2000. Méthode couplée éléments spectraux – solution modale pour la propagation d'ondes dans la Terre à l'échelle globale, *PhD thesis,* Université Paris 7.

Capdeville, Y., 2009. Procédé de détermination d'un modéle élastique effectif. Brevet FR 09 57637, filed on the Otcober 29th 2009.

Capdeville, Y. & Marigo, J.J., 2007. Second order homogenization of the elastic wave equation for non-periodic layered media, *Geophys. J. Int.,* **170,** 823–838.

Capdeville, Y. & Marigo, J.J., 2008. Shallow layer correction for spectral element like methods, *Geophys. J. Int.,* **172,** 1135–1150.

Chaljub, E., Komatitsch, D., Capdeville, Y., Vilotte, J.-P., Valette, B. & Festa, G., 2007. Spectral element analysis in seismology, in *Advances in Wave Propagation in Heterogeneous Media,* Vol. 48, pp. 365–419, eds Wu, R.-S. & Maupin, V., Advances in Geophysics Series, Elsevier.

Chapman, C., 2004, *Fundamentals of Seismic Wave Propagation,* Chapter 7, pp. 274–276. Cambridge University Press, Cambridge.

Dumontet, H., 1986. Study of a boundary layer problem in elastic composite materials, *RAIRO Modél. Math. Anal. Numér.,* **20**(2), 265–286.

Fish, J. & Chen, W., 2004. Space-time multiscale model for wave propagation in heterogeneous media, *Comp. Meth. Appl. Mech. Engng,* **193,** 4837–4856.

Fish, J., Chen, W. & Nagai, G., 2002. Nonlocal dispersive model for wave propagation in heterogeneous media. Part 1: one-dimensional case, *Int. J. Numer. Methods Engrg.,* **54,** 331–346.

Fogarty, T. & LeVeque, R.J., 1999. High-resolution finite volume methods for acoustics in periodic or random media, *J. acoust. Soc. Am.,* **106,** 17–28.

Francfort, G.A. & Murat, F., 1986. Homogenization and optimal bounds in linear elasticity, *Arch. Rational Mech. Anal.,* **94**(4), 307–334.

Haboussi, M., Dumontet, H. & Billoët, J., 2001a. On the modelling of interfacial transition behavior in composite materials, *Comput. Mater. Sci.,* **20,** 251–266.

Haboussi, M., Dumontet, H. & Billoët, J., 2001b. Proposed of refined interface models and their application for free-edge effect interface modelling in laminated composites for free edge effect analysis, *Composit. Interfaces,* **8**(1), 93–107.

Hornung, U., 1996. *Homogenization and Porous Media,* Springer.

Hughes, T.J.R., 1987. *The Finite Element Method, Linear Static and Dynamic Finite Element Analysis,* Prentice-Hall International, Englewood Cliffs, NJ.

Komatitsch, D. & Vilotte, J.P., 1998. The spectral element method: an effective tool to simulate the seismic response of 2D and 3D geological structures, *Bull. seism. Soc. Am.,* **88,** 368–392.

Komatitsch, D., Martin, R., Tromp, M.A., Taylor, J. & Wingate, B.A., 2001. Wave propagation in 2-D elastic media using a spectral element method with triangles and quadrangles, *J. Comput. Acoust.,* **9,** 703–718.

Kaser, M. & Dumbser, M., 2006. An arbitrary high-order discontinuous galerkin method for elastic waves on unstructured meshes -I. the two-dimensional isotropic case with external source terms, *Geophys. J. Int.,* **166,** 855–877.

Lurie, K.A., 2009. On homogenization of activated laminates in 1D-space and time, *Z. Angew. Math. Mech.,* **4,** 333–340.

Marchenko, V.A. & Khruslov, E.Y., 2005, *Homogenization of Partial Differential Equations,* Vol. 46: Progress in Mathematical Physics, Birkhäuser, Boston.

Mercerat, E.D., Vilotte, J.P. & S´nchez-Sesma, F.J., 2006. Triangular spectral element simulation of two-dimensional elastic wave propagation using unstructured triangular grids, *Geophys. J. Int.,* **166,** 679–698.

Milton, G.W. & Willis, J.R., 2007. On modifications of newton's second law and linear continuum elastodynamics, *Proc. R. Soc. A,* **463,** 855–880.

Moczo, P., Kristek, J., Vavryčuk, V., Archuleta, R.J. & Halada, L., 2002. 3D heterogeneous staggered-grid finite-difference modeling of seismic motion with volume harmonic and arithmetic averaging of elastic moduli and densities, *Bull. seism. Soc. Am.,* **92**(8), 3042–3066.

Moskow, S. & Vogelius, M., 1997. First-order corrections to the homogenised eigenvalues of a periodic composite medium. A convergence proof, *Proc. Roy. Soc. Edinburgh Sect. A,* **127**(6), 1263–1299.

Murat, F. & Tartar, L., 1985. Calcul des variations et homogénéisation. In *Homogenization Methods: Theory and Applications in Physics (Bréausans-Nappe, 1983),* Vol. 57: Collect. Dir. Études Rech. Élec. France, pp. 319–369. Eyrolles, Paris.

Nguetseng, G., 2003. Homogenization structures and applications I, *Z. Anal. Anw.,* **22,** 73–107.

Papanicolaou, G.C. & Varadhan, S., 1979. Boundary value problems with rapidly oscillating random coefficients, in *Proceedings of Conference on Random Fields, Esztergom, Hungary, 27,* Seria Colloquia Mathematica Societatis Janos Bolyai, pp. 835–873. North Holland, Amsterdam.

Parnell, W. & Abrahams, I., 2006. Dynamic homogenization in periodic fibre reinforced media, Quasi-static limit for SH waves, *Wave Motion,* **43,** 474–498.

Priolo, E., Carcione, J.M. & Seriani, G., 1994. Numerical simulation of interface waves by high-order spectral modeling techniques, *J. acoust. Soc. Am.,* **95**:2, 681–693.

Sanchez-Palencia, E., 1980, *Non-homogeneous Media and Vibration Theory,* Number 127 in Lecture Notes in Physics. Springer, Berlin.

Seriani, G., 1997. A parallel spectral element method for acoustic wave modeling, *J. Comput. Acoust.,* **5,** 53–69.

Seriani, G., 1998. 3-D large-scale wave propagation modeling by a spectral element method on a Cray T3E multiprocessor, *Comput. Methods Appl. Mech. Engrg.,* **164,** 235–247.

Willis, J.R., 1981. Variational principles for dynamic problems for inhomogeneous elastic media, *Wave Motion,* **3,** 1–11.

Zhang, C. & LeVeque, R.J., 1997. The immersed interface method for acoustic wave equations with discontinuous coefficients, *Wave Motion,* **25,** 213–302.

APPENDIX A:

We show here that $E^{\rho*} = \langle \rho \chi^1 \rangle$. We start with

$$\partial_y [E \partial_y \chi^\rho] = \rho - \langle \rho \rangle. \tag{A1}$$

Multiplying the last equation by χ^1, taking the cell average and using the fact that $\langle \chi^1 \rangle = 0$, we find

$$\langle \chi^1 \partial_y \left[E \partial_y \chi^\rho \right] \rangle = \langle \chi^1 \rho \rangle . \tag{A2}$$

Using an integration by part, we have

$$- \langle \partial_y \chi^1 \left[E \partial_y \chi^\rho \right] \rangle = \langle \chi^1 \rho \rangle . \tag{A3}$$

Using (24) we find

$$\langle E \partial_y \chi^\rho \rangle = \langle \chi^1 \rho \rangle , \tag{A4}$$

which, using the definition $E^{\rho*} = \langle E \partial_y \chi^\rho \rangle$, is the wanted result.